Mössbauer effect study on the mixed valence state of iron in tourmaline

E. A. FERROW
Department of Mineralogy and Petrology, University of Lund, Sölvegatan 13, S-222 62 Lund, Sweden
H. ANNERSTEN
Department of Mineralogy and Petrology, University of Uppsala, Box 555, S-751 22 Uppsala, Sweden
AND
R. P. GUNAWARDANE
Department of Chemistry, University of Paradeniya, Paradeniya, Sri Lanka

Abstract

Mössbauer spectra of iron-bearing tourmaline, obtained at different temperatures, show the existence of thermally-activated charge delocalization among clusters of iron atoms situated in the *Y* and *Z* octahedra of the tourmaline structure. The temperature dependence indicates an unusually high activation energy for the delocalization process which suggests that the process takes place between crystallographically non-equivalent sites. Annealing of the tourmaline in hydrogen is observed to inhibit the delocalization process, thus localizing the electron into the Z-site.

KEYWORD: Mössbauer effect, tourmaline, iron, charge delocalization, Sweden, H_2 annealing.

Introduction

THE crystal chemistry of tourmaline is very complex. Even though some progress has been achieved in understanding its crystal chemistry, a number of conflicting observations have been reported in the literature. For example, Iijima *et al.* (1973), using high resolution transmission electron microscopy (HRTEM), demonstrated that Fe^{2+}-rich tourmaline shows a high degree of ordering and a plane-group symmetry that differs from Fe^{3+}-rich tourmaline, a result that contradicts X-ray diffraction structure analysis. They suggested electron irradiation as a possible mechanism for cation ordering, but realized that this is not an entirely satisfactory explanation. Recently, Smith (1978), using optical spectroscopy, studied a variety of tourmalines under different conditions and found that oxidation and reduction take place simultaneously on annealing iron-bearing tourmalines in hydrogen. However, he could not suggest any reaction mechanism for his observations. It is difficult to imagine the oxidation of iron in a reducing environment and we found it necessary to (1) check the observations of Smith by techniques other than optical spectroscopy, (2) explore possible reaction mechanisms for such an oxidation–reduction process, and (3) look for a relation between the observation of Iijima *et al.* (1973) and that of Smith (1978). To this end we have investigated the behaviour of iron in tourmalines under different redox conditions using the Mössbauer effect (ME), electron-probe microanalysis, powder X-ray diffraction (XRD), differential thermal analysis (DTA) and thermogravimetric analysis (TGA).

Crystal chemistry of tourmaline

The tourmaline group of minerals is well known for its wide range of composition. Tourmaline may be represented by the general formula $XY_3Z_6B_3Si_6O_{27}(OH,F)_4$ and crystallizes in space group *R3m*. The *X*-site is usually occupied by large cations such as Na^+, K^+, Ca^{2+}, while smaller cations such as Li, Al, Mg, and Fe occupy the *Y*-site. The *Z*-site is chiefly occupied by Al, but it has been shown that Fe can replace Al in this site (Barton, 1969). Commonly recognized end members are dravite, schorl and elbaite with Mg, Fe, and Li/Al in the *Y* position, respectively.

Mineralogical Magazine, April 1988, Vol. 52, pp. 221–228

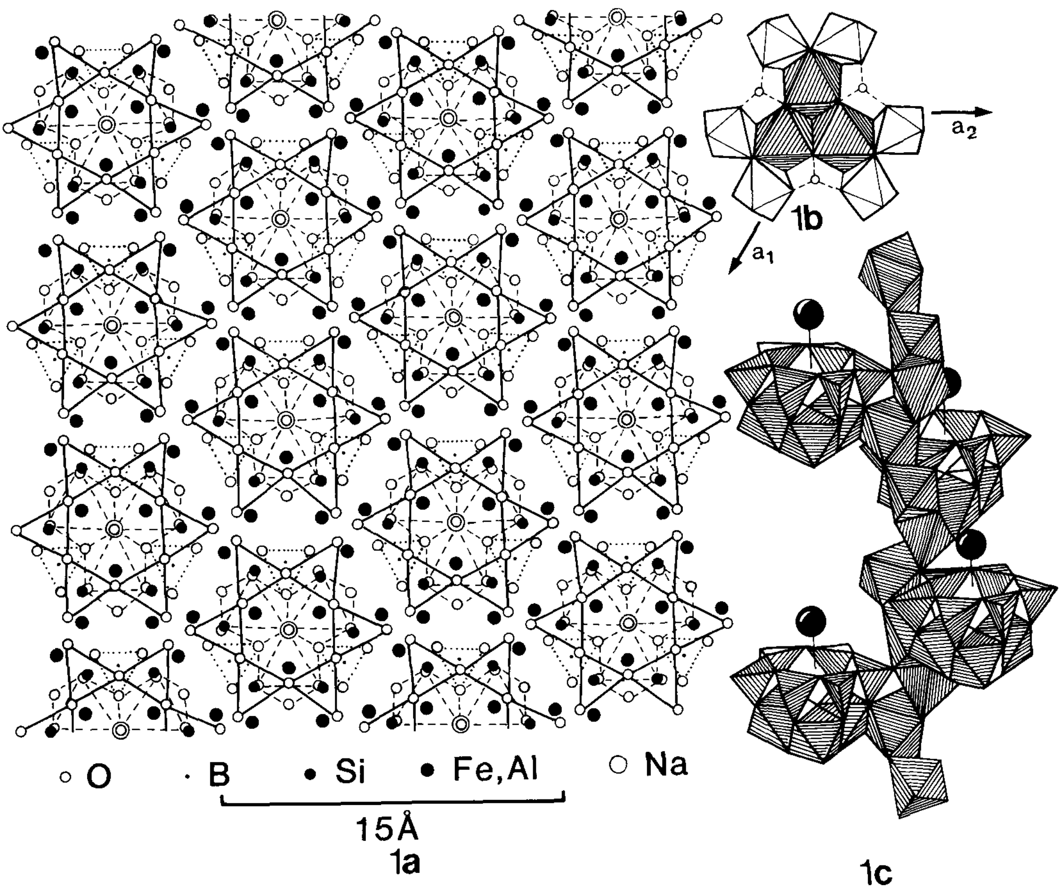

FIG. 1(*a–c*). Structure of tourmaline: (*a*) (0001) projection showing a plane of regular hexagonal SiO_4 tetrahedra (from Iijima *et al.*, 1973); (*b*) fragment from the *Y*-octahedra (shaded) forming trigonal planar clusters perpendicular to the *c*-axis with nearby *Z*-octahedra (unshaded); (*c*) winding spiral bands of *Z*-octahedra in the crystallographic *c* direction. Note that each *Y*-site octahedron shares edges with two more *Y*-site octahedra and two *Z*-site octahedra (1*b*). Furthermore, each *Z*-site octahedron shares two edges with other *Z*-site octahedra (1*c*), (from Korovushkin *et al.*, 1979).

Complete series of solid solution exist between the end members, except in the case of the two Fe-free forms.

The detailed structure of different tourmalines has been investigated by many workers (Donnay and Buerger, 1950; Barton, 1969; Donnay and Barton, 1972; Fortier and Donnay, 1975). In tourmaline, SiO_4 tetrahedra arê arranged in regular hexagonal rings in a plane (Fig. 1*a*). Below this plane there is a sheet of octahedra in which two types of octahedra are recognized. The three large central octahedra are occupied by *Y* cations while pairs of smaller octahedra share edges with the central *Y* octahedra and are occupied by *Z* cations. The boron atom helps to bind together the octahedral layers and is coordinated to three oxygen atoms (Fig. 1*b*). The larger, brucite-type, *Y* octahedra are coordinated by four oxygen and two hydroxyl anions, while the smaller and more distorted *Z* octahedra are coordinated by five oxygen and one hydroxyl anions. The two have $C_s(m)$ and $C_1(1)$ point symmetries, respectively. The most interesting feature observed in the structure of tourmaline is that two octahedra possessing different symmetries and sizes share edges. Each *Y*-site octahedron shares a total of four edges with two adjacent *Y* and two adjacent *Z* octahedra. Furthermore, each *Z*-site octahedron shares two edges with adjacent *Z*-site octahedra connected in the form of a single spiral (Fig. 1*c*).

Experimental

A naturally occurring pegmatitic tourmaline from Örnö, Central Sweden, was analysed by electron microprobe, optical microscope and XRD (Table 1). The mineral showed no chemical or optical zoning and in thin section it exhibited marked pleochroism with blue–green to faint brown colouration. The ME spectra of the specimen and its hydrogen-reduced derivative were obtained at different temperatures using conventional techniques as described in detail by Annersten *et al.* (1982).

Table 1. Microprobe analysis and unit cell parameters of tourmaline from Örnö, Central Sweden.

		Cell Data (Å)			
	Wt %	a	c	V	Remarks
SiO_2	37.23	15.96(2)	7.16(7)	1581 (5)	original
Al_2O_3	8.80	15.94(3)	7.17(8)	1580 (1)	H_2 annealed
FeO	3.45				
Fe_2O_3	1.17				
MgO	4.39				
Na_2O	1.84				
TiO_2	0.23				
MnO	0.20				
CaO	0.05				
Total	87.42				

FeO/Fe_2O_3 from Mössbauer data. Li, B, H_2O and F not included.

Crystal chemical changes occurring in the samples were investigated using a Differential Scanning Calorimeter model DSS-2C in the temperature range 300–800 K. Thermogravimetric analysis TGA was carried out using a Perkin-Elmer Thermogravimetric Analyser model TGS-2 in the same temperature range.

Results

ME spectra of tourmaline and its H_2 annealed product were obtained at different temperatures between 77 and 807 K and the results from the computer fits are shown in Table 2 and Figs. 2 and 3. Only the high-velocity components of the absorption doublets are resolved in the figures.

Assignment of the two ferrous iron doublets is done in accordance with Burns (1972), with the outer doublet due to Fe^{2+} in the Y position and the inner, less intense doublet due to Fe^{2+} in the Z position. In the 77 K spectrum two fitting models were tried, one with all the ferric iron in the Y site and the other with ferric iron in both Y and Z sites. The results suggest that Fe^{3+} dominates one site only (Fig. 2*a*), probably the Y site as demonstrated from optical studies by Mattson and Rossman (1984). The spectrum obtained at room temperature show a broad envelope between the dominating high- and low-energy components of the ferrous iron (Fig. 2*b*). Although no separate absorption lines could be resolved, a fit with a minimum of three doublets could reasonably account for the broadening. The ME parameters (especially the isomer shift, which is sensitive to the electron density around the iron nuclei) for these three doublets indicate values that are intermediate between those of Fe^{2+} and Fe^{3+} and are assigned to iron with non-integral oxidation state, Fe^{2n+} (see Saegusa *et al.*, 1978). At elevated temperatures, 525 K, the envelope narrows and this could be fitted with only two doublets (Fig. 2*c*) and at still higher temperature, 807 K, the broad envelope is fully lost and only one doublet with a line width of 0.38 mm/s could be resolved (Fig. 2*d*). This process is reversible and the original spectrum was obtained when the absorber was brought down to room temperature. From the intensity ratios of the absorption doublets, it is very important to point out that at all temperatures the oxidation ratio, $Fe^{3+}/(Fe^{2+} + Fe^{3+})$, and the total integrated intensity of the non-integral iron, Fe^{2n+}, remain constant, indicating that no oxidation or reduction took place (Table 2).

The room-temperature ME spectrum of tourmaline annealed in hydrogen at 750 K shows quite a different feature (Fig. 3*a*). The spectrum shows that, compared with the original untreated sample (Fig. 2*b*), there is an increase in intensity of both the ferric iron and the inner ferrous iron at the expense of the broad envelope which is reduced in intensity by 11%, an amount comparable to the total increase of the ferric and ferrous iron intensities. Measurement of the annealed sample at 674 K (Fig. 3*b*) shows the same narrowing of the remaining envelope as was observed in Fig. 2, and no oxidation or reduction took place. The heating process is reversible and the spectrum shown in Fig. 3*a* is obtained when the temperature

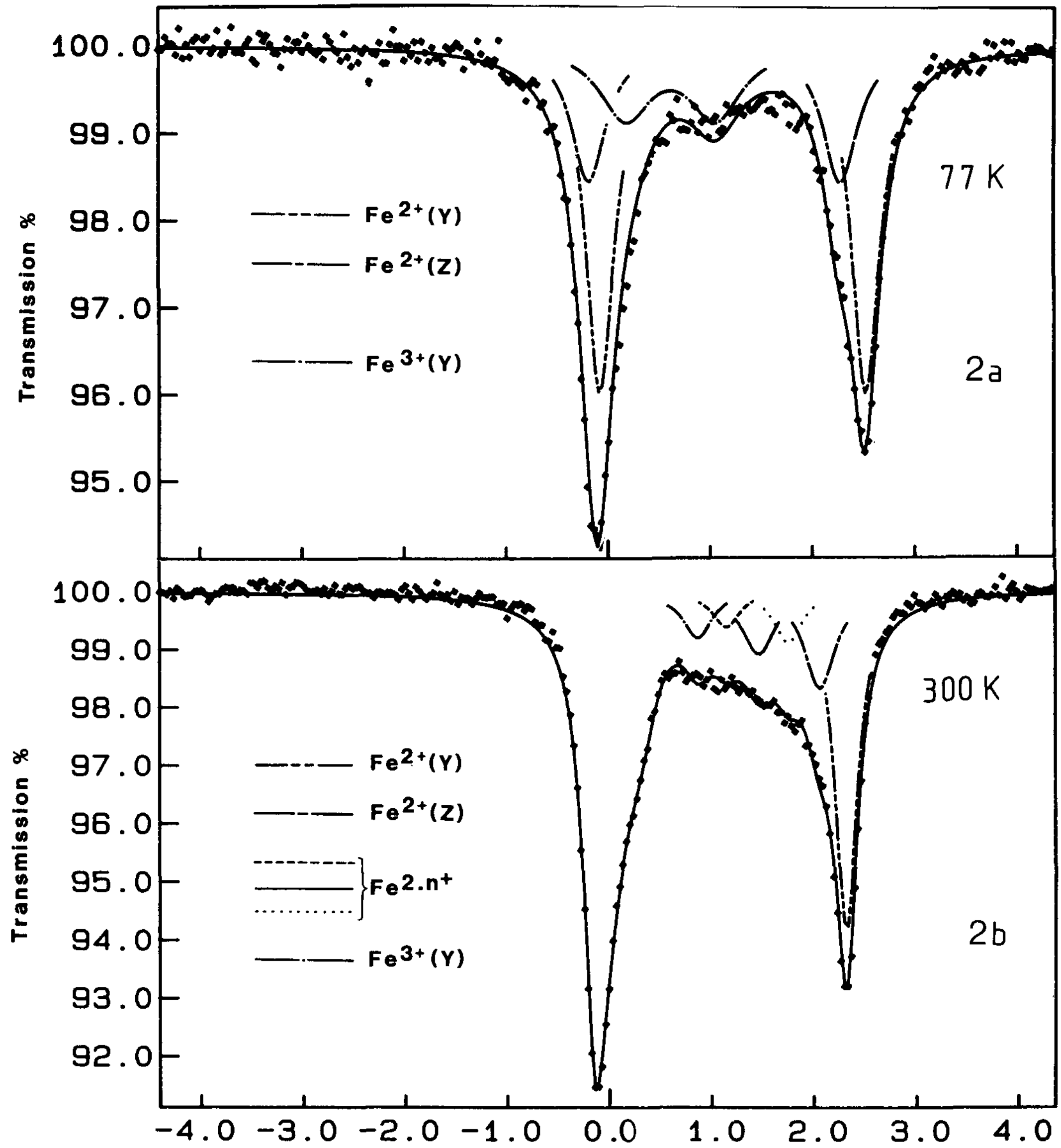

FIG. 2(*a–d*). ^{57}Fe Mössbauer spectra of tourmaline from Örnö, Central Sweden, at different temperatures. For convenience only the high-velocity components of the doublets are shown. Note that at both low temperature (*a*) and high temperature (*d*) the broad absorption envelope observed at room temperature disappears, but the oxidation ratio remains constant (Table 2).

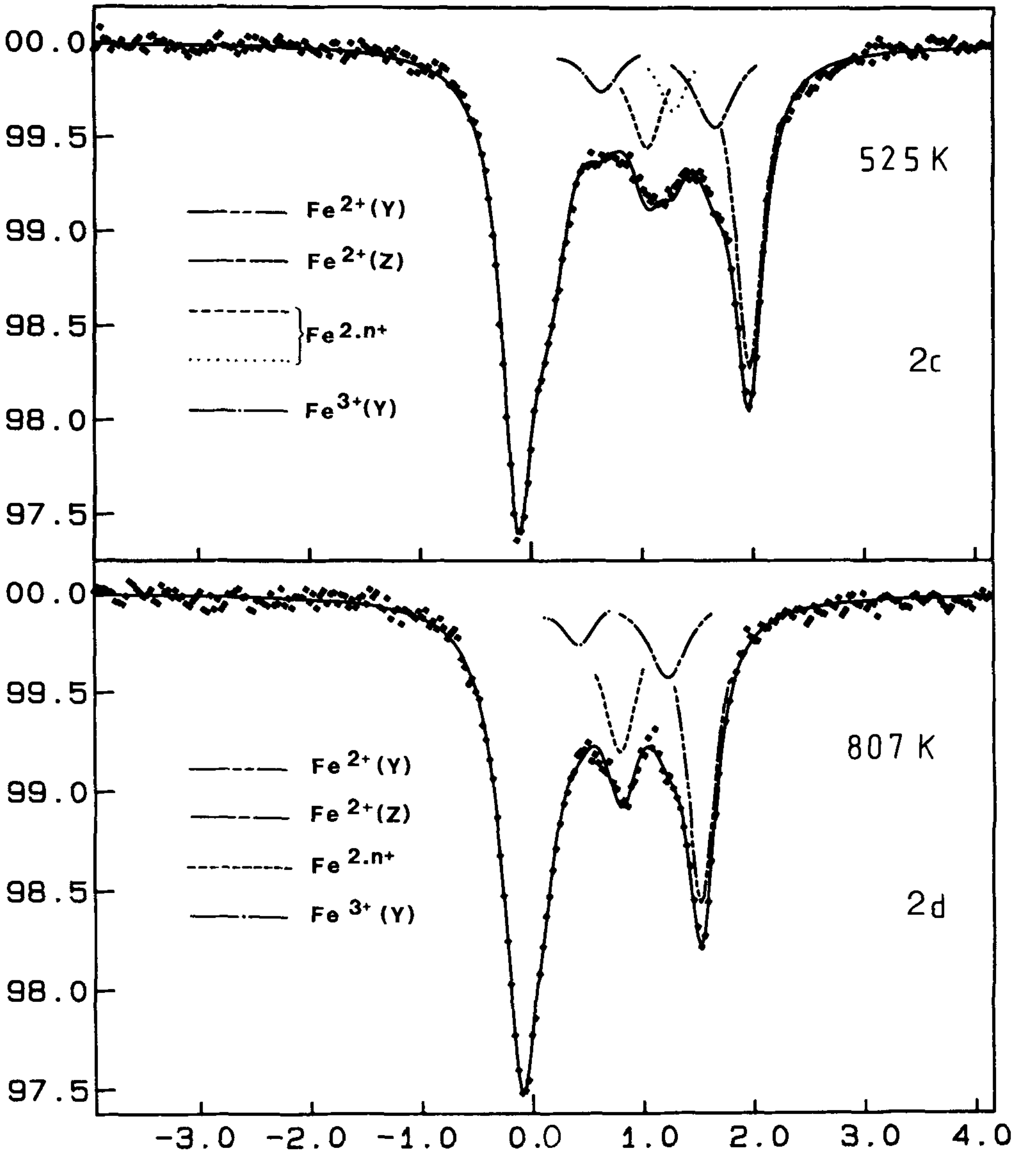
00.0
99.5
99.0
98.5
98.0
97.5
525 K
2c
Fe 2+(Y)
Fe 2+(Z)
Fe 2.n+
Fe 3+(Y)
807 K
2d
-3.0
-2.0
-1.0
0.0
1.0
2.0
3.0
4.0

Table 2. Mössbauer parameters of tourmaline from Örnö at different temperatures.

T(K)	CS	QS	W	Area	Assignment
77	1.23	2.62	0.33	0.54	Fe^{2+}(Y)
	1.04	2.47	0.41	0.24	Fe^{2+}(Z)
	0.55	0.75	0.51	0.22	Fe^{3+}(Y)
300	1.09	2.48	0.27	0.46	Fe^{2+}(Y)
	1.01	2.10	0.37	0.18	Fe^{2+}(Z)
	0.89	1.63	0.34	0.09	$Fe^{2.n+}$
	0.81	1.21	0.39	0.13	$Fe^{2.n+}$
	0.71	0.75	0.33	0.06	$Fe^{2.n+}$
	0.37	0.88	0.34	0.08	Fe^{3+}(Y)
525	0.92	2.10	0.30	0.46	Fe^{2+}(Y)
	0.81	1.61	0.44	0.17	Fe^{2+}(Z)
	0.76	1.05	0.32	0.10	$Fe^{2.n+}$
	0.58	0.92	0.36	0.17	$Fe^{2.n+}$
	0.21	0.85	0.38	0.09	Fe^{3+}(Y)
807	0.72	1.62	0.31	0.46	Fe^{2+}(Y)
	0.54	1.40	0.44	0.18	Fe^{2+}(Z)
	0.45	0.69	0.38	0.27	$Fe^{2.n+}$
	0.09	0.67	0.38	0.09	Fe^{3+}(Y)
	After annealing in hydrogen				
300	1.09	2.41	0.33	0.38	Fe^{2+}(Y)
	1.05	1.82	0.43	0.30	Fe^{2+}(Z)
	1.01	1.32	0.29	0.06	$Fe^{2.n+}$
	0.68	1.20	0.44	0.10	$Fe^{2.n+}$
	0.36	0.96	0.36	0.16	Fe^{3+}(Y)
674	0.80	1.64	0.42	0.39	Fe^{2+}(Y)
	0.64	1.35	0.49	0.28	Fe^{2+}(Z)
	0.55	0.73	0.36	0.16	$Fe^{2.n+}$
	0.13	0.73	0.36	0.17	Fe^{3+}(Y)

CS = centroid shift relative to metallic iron (±0.01mm/s)

QS = quadrupole splitting (±0.01mm/s)

W = full width at half maximum in mm/s

$Fe^{2.n+}$ refers to the non-integral iron where the extra electron is delocalized.

of the absorber is brought down to 300 K, while the change observed by annealing in hydrogen is not.

No thermal transitions or crystal–chemical changes were observed in the original and hydrogen-annealed samples from DTA, TGA and microprobe studies in the temperature range 300–800 K. A slight increase in *c*-axis (0.01 Å) and a slight decrease in *a*-axis and volume (0.02 Å and 1.4 Å^3, respectively) was observed after annealing the sample in H_2 (Table 1).

Discussion

We assign the broad envelope between the high velocity Fe^{2+} and Fe^{3+} absorption peaks in the room-temperature spectrum (Fig. 2*b*) to delocalized electrons around iron. Similar features have been observed in Zn–Ti–Fe spinels (Lotgering and van Diepen, 1977), where the continuous absorption band has been assigned to thermally activated charge delocalization between chemically non-equivalent *B*-sites in spinels. By considering an Fe^{3+}–Fe^{2+} pair as two Fe^{3+} cores with an itinerant electron, the non-equivalence between two sites (chemical or crystallographical) can be represented by a difference in potential energy. The energy of activation, i.e. the energy required by the electron to overcome the potential difference, is proportional to the lattice vibration frequency, temperature and population fraction of the itinerant electrons in the site with lower potential (cf. Lotgering and van Diepen, 1977). Compared to spinels, line broadening of the non-integral absorption doublet is observed at still higher temperatures in tourmaline. This indicates a much higher energy of activation for the electron exchange process, suggesting that charge delocalization takes place between different crystallographic sites. This is supported by the result on the hydrogen-annealed sample in which we observe simultaneous increase in intensity of ferric and ferrous iron absorption doublets in the *Y* and *Z* positions respectively, together with a decrease of the broad absorption envelope assigned to the non-integral iron. Fe–Fe interaction occurs between the two octahedral sites according to:

$$Fe^{2+}(Y) + Fe^{3+}(Z) \rightleftharpoons Fe^{3+}(Y) + Fe^{2+}(Z) \quad (1)$$

The role of hydrogen in the process is not clear. It seems to have no chemical effect on the high oxidation state of iron as expected, i.e. no protonation takes place. It shows, however, that H_2 annealing favours the forward reaction in equation (1). We suggest that hydrogen in the structure

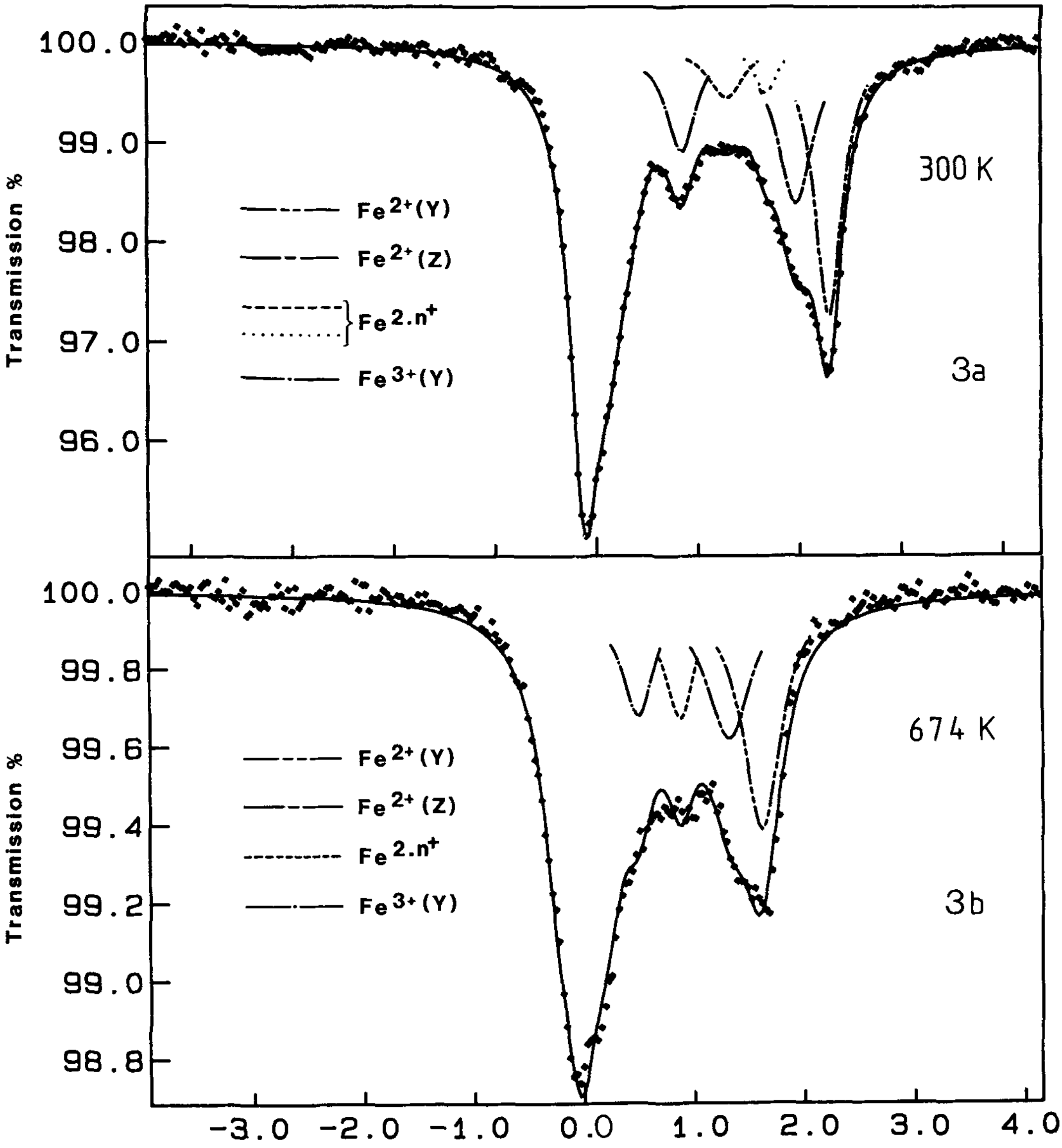

FIG. 3. ^{57}Fe Mössbauer spectra at two temperatures of tourmaline annealed in hydrogen at 750 K. Compare the room temperature spectra of Figs. 2 and 3 (2*b* and 3*a*) to see the effect of H_2 annealing where Fe^{3+} is ordered in the *Y* site and Fe^{2+} in the *Z* site.

of tourmaline may cause a polarization effect, reducing the delocalization of the electrons.

The model proposed for the above reaction is based on the ability of tourmaline to adjust its structure to different chemical environments. Hermon *et al.* (1973), for example, have shown that, in order to produce matching along the shared edge of the chemically and crystallographically distinct *Y* and *Z* coordination polyhedra, the average effective cationic radii must have the proper size relation to each other. Cations of multiple oxidation state and variable ionic radii (iron, for example) take adjacent *Y* and *Z* positions as isolated domains with Fe^{2+}–Fe^{3+} pairs in which electron delocalization takes place, an idea recently suggested by Mattson and Rossman (1987). The broadening observed at decreasing temperatures reflects the decrease in hopping frequency within different domains. Annealing in hydrogen inhibits the electron delocalization and forces the itinerant electron to be localized in one of the two octahedral sites. This results in iron of integral valence states (Fe^{2+} and Fe^{3+}) while the total oxidation ratio remains constant. This ordering of Fe^{3+} in the *Y*-site and Fe^{2+} in the *Z*-site on annealing in hydrogen is also observed by optical spectroscopy (Smith, 1978). The site of localization of the electron is controlled by structural factors where a better fit is obtained along the shared edge if the bigger Fe^{2+} is accommodated in the smaller *Z*-site. The cation ordering observed in tourmaline by TEM (Iijima *et al.*, 1973) can be explained in a similar way, where the electron microscope column with its electron beam serves as a reducing environment and in an analogous manner inhibits electron delocalization and stabilizes the forward reaction of equation (1). The discrepancy observed in symmetry between TEM images and XRD structural analyses of Fe^{2+}-rich tourmaline is simply a reflection of the difference in ME spectra before and after annealing of tourmaline in hydrogen (Figs. 2*b* and 3*a*, respectively). In Fe^{3+}-rich ones where Fe^{2+}–Fe^{3+} domains are few, charge delocalization is limited and electron-induced cation ordering is not very pronounced.

In conclusion, factors that govern electron delocalization in minerals have been discussed by Nolet and Burns (1979) and Amthauer and Rossman (1984). In addition to their findings, thermally activated electron delocalization in tourmaline is observed between crystallographically non-equivalent co-ordination polyhedra. The relatively high temperature needed for this process, 500–800 K, indicates a high activation energy which reflects the asymmetry of the two octahedral sites involved in the electron transfer. Furthermore, annealing in hydrogen inhibits charge delocalization whereby the itinerant electron is localized on the *Z*-site. The role of hydrogen is not clear but the electron beam in a TEM seems to have the same effect.

Acknowledgments

We are grateful to Drs Roger Burns, George Rossman, Gabrielle Donnay, and Ulf Hålenius for critical review of the manuscript. We also acknowledge the review of the anonymous referee. One of us (RPG) wishes to thank the International Seminar on Chemistry and Physics of the University of Uppsala for granting a fellowship. The work was financed by the Swedish Natural Science Research Council (NFR).

References

Amthauer, G. and Rossman, R. G. (1984) Mixed valence state of iron in minerals with cation cluster. *Phys. Chem. Minerals* **11**, 37–51.

Annersten, H., Ericsson, T. and Filippidis, A. (1982) Cation ordering in Ni–Fe olivines. *Am. Mineral.* **67**, 1212–7.

Barton, R. Jr. (1969) Refinement of the crystal structure of buergerite and the absolute orientation of tourmaline. *Acta Crystallogr.* **25**, 1523–33.

Burns, R. G. (1972) Mixed valencies and site occupancies of iron in silicate minerals from Mössbauer spectroscopy. *Can. J. Spectroscopy* **17**, 251–9.

Donnay, G. and Barton, R. Jr. (1972) Refinement of the crystal structure of elbaite and the mechanism of tourmaline solid solution. Tchermaks. *Mineral. Petrpg. Mitt.* **18**, 273–86.

——and Buerger, M. J. (1950) The determination of the crystal structure of tourmaline. *Acta Crystallogr.* **3**, 379–88.

Fortier, S. and Donnay, G. (1975) Schorl refinement showing composition dependence of the tourmaline structure. *Can. Mineral.* **13**, 173–7.

Hermon, E., Simkin, D. J., Donnay, G. and Muir, W. B. (1973) The distribution of Fe^{2+} and Fe^{3+} in the iron-bearing tourmaline: A Mössbauer study. *Tchermaks Mineral. Petrog. Mitt.* **19**, 124–32.

Iijima, S., Cowley, J. M. and Donnay, G. (1973) High resolution electron microscopy of tourmaline crystals. Ibid. **20**, 216–24.

Korovushkin, V. V., Kuzmin, V. I. and Belov, V. F. (1979) Mössbauer studies of structural features in tourmaline of various genesis. *Phys. Chem. Minerals* **4**, 209–20.

Lotgering, F. K. and van Diepen, A. M. (1977) Electron exchange between $^{2+}$ and Fe^{3+} on octahedral sites in spinels studied by means of paramagnetic and Mössbauer spectra and susceptibility measurements. *J. Phys. Chem. Solids* **38**, 565–72.

Mattson, S. M. and Rossman, G. R. (1984) Ferric iron in tourmaline. *Phys. Chem. Minerals* **11**, 225–34.

————(1987) Fe^{2+}-Fe^{3+} interaction in tourmaline. Ibid. **14**, 163–71.

Nolet, D. A. and Burns, R. G. (1979) A study of the temperature-dependent electron delocalization by the Mössbauer Effect. Ibid. **4**, 221–34.

Saegusa, N., Price, D. C. and Smith, G. (1978) Analysis of the Mössbauer spectra of several iron-rich tourmalines. *International conference on the application of the Mössbauer effect.* Kyoto, Japan.

Smith, G. (1978) A reassesement of the role of iron in the 5000–30 000 cm^{-1} region of the electron absorption of tourmaline. *Phys. Chem. Minerals* **3**, 343–73.

[*Manuscript received 2 December 1986: revised 6 April 1987*]